scientific commentaries

Coordination chemistry of anions through halogen-bonding interactions

Marc Fourmigué*

Institut des Sciences Chimiques de Rennes (ISCR), Université de Rennes 1 and CNRS, Campus de Beaulieu, 35042 Rennes, France. *Correspondence e-mail: marc.fourmigue@univ-rennes1.fr

While an IUPAC definition for hydrogen bonding was only released in 2011 after decades of discussions in the scientific community (Arunann *et al.*, 2011), it did not take such a long time to come up with an analogous definition of halogen bonding (Desiraju *et al.*, 2013), following a revival of this interaction in the literature, which can be traced back to the early 1990s. The identification of this interaction is, however, not recent, as illustrated by the isolation of the $H_3N \cdot I_2$ adduct (Colin, 1814). Two centuries later, several review articles (Cavallo *et al.*, 2016; Gilday *et al.*, 2015; Fourmigué, 2009) have gathered together most available data. The halogen-bonding interaction (noted XB) is essentially described as an electrostatic interaction between a charge concentration (Lewis base) and a charge-depleted area, called an σ-hole, that a covalently bound halogen atom exhibits in the extension of this bond. Note that a charge-transfer covalent contribution can be found in the strongest halogen bonds, as illustrated for example in the triiodide anion following: $I_2 + I^- \rightarrow (I-I-I)^-$. The presence of a halogen bond is characterized by a shortening of the interatomic distance, relative to the sum of the van der Waals (or ionic) radii of the interacting atoms, which is defined as the reduction ratio. The halogen-bond donor character of halogenated molecules is modulated by the nature of the halogen with I > Br >> Cl >> F, by the hybridization of the substituted C atom with $C\equiv C-I$ > $C=CH-I$ > $C-CH_2-I$, and by the electron-withdrawing ability of the carbon substituents, with a strong activation in aliphatic and aromatic perfluorinated substrates such as $F_{2n+1}C_n-I$ or $C_6F_{6-n}I_n$. Besides, dihalogens (I_2, Br_2, Cl_2), interhalogens (I—Cl, I—CN) and *N*-iodoimides (*N*-iodosuccinimide, *N*-iodosaccharin) are also strong halogen-bond donors. All Lewis bases are potentially XB acceptors and among them, anionic species, and particularly halide anions (Cl^-, Br^-, I^-) thanks to a maximal charge concentration (Metrangolo *et al.*, 2008*a*; Cavallo *et al.*, 2010).

The paper by Szell *et al.* (2017) in this special issue of *Acta Crystallographica Section B* deals with such a crystal engineering approach through the formation of co-crystals associating ammonium or phosphonium halide salts with neutral, halogenated, activated halogen-bond donors such as *sym*-triiodotrifluorobenzene (1) or more specifically here its extended analog, 1,3,5-tris(iodoethynyl)-2,4,6-trifluorobenzene) (2). While ditopic halogen-bond donors such as diiodoacetylene (I—C≡C—I) or *para*-diiodotetra-fluorobenzene most often lead to one-dimensional systems in the presence of halide anions, it was expected that threefold symmetric molecules such as (1) or (2) would provide higher symmetry structures (trigonal, hexagonal, cubic) that would express the molecular threefold symmetry of the halogen-bond donor.

Earlier reports (Metrangolo *et al.*, 2008*b*) have indeed shown that 'the mutual induced fitting process elicits the tridentate coordination profile of both 1,3,5-trifluoro-2,4,6-triiodobenzene (1) and I^- ions resulting in cation-templated anionic (6,3) networks', with the small cations (Me_3S^+, Me_4P^+, Et_4N^+) sitting within the pores of the honeycomb network. With $Et_4N^+I^-$, $Et_4P^+I^-$ and solid solutions thereof, the adducts even crystallize in the trigonal space group $R\bar{3}c$, while with larger cations (Metrangolo *et al.*, 2008*b*; Triguero *et al.*, 2008), the (6,3) networks were maintained but strongly corrugated. In a search for larger pores, the extended halogen-bond donor (2) was recently designed (Lieffrig *et al.*, 2013) and further used here with another set of cations of varying size and shape (Szell *et al.*, 2017). Remarkably, besides the above-described honeycomb networks with tricoordinated halide anions (Fig. 1*a*), the adduct with the larger $EtPh_3P^+Br^-$ salt crystallizes in the cubic space group $Pa\bar{3}$, with sixfold coordination around the bromide anion (Fig. 1*c*), as already observed with the smaller $Et_3BuN^+Br^-$ salt (Lieffrig *et al.*,
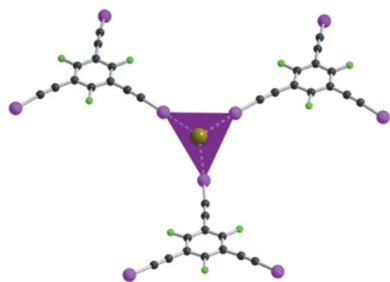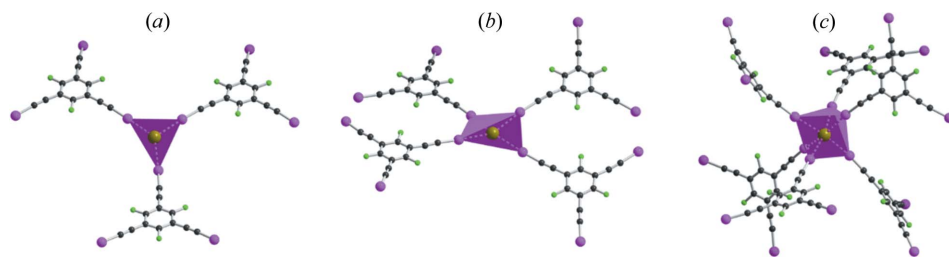
Figure 1
Detail of the coordination spheres of the bromide anion in three adducts of (2) with: (a) $Et_3BuN^+Br^-$, (b) $MePh_3P^+Br^-$ and (c) $EtPh_3P^+Br^-$.

2013) which crystallizes in the cubic space group $Ia\bar{3}$. Furthermore, the XB interaction of acetonitrile acting as XB acceptor toward one iodine atom of (2) leaves only two I atoms (out of three) to interact with the halide anion, and leads to another set of structures with a four-coordinated bromide anion (Fig. 1b).

These beautiful examples illustrate a charge-inverted coordination chemistry, where the metal cation is replaced by the halide anion and where the ligands are replaced by the halogen-bond donors. The essentially electrostatic nature of the XB interaction has important consequences on the coordination number and geometry. Indeed, in classical coordination chemistry, the overlap interactions of the ligand's orbitals with the nd, $(n + 1)s$ and $(n + 1)p$ orbitals of the metal center, together with the electron count, determines the favored coordination number and geometry. This does not hold in the present situation, where many examples exhibit very acute $I \cdots X^- \cdots I$ angles, as observed for example in the dicoordinated bromide anion (74°) in the one-dimensional chains formed from *para*-diiodotetrafluorobenzene adduct with $Me_4N^+Br^-$ (Grebe *et al.*, 1999), or with the tricoordinated bromide anion in the honeycomb network formed from $Bu_4N^+Br^-$ and (2) (Lieffrig *et al.*, 2013), where the sum of the three $I \cdots Br^- \cdots I$ angles does not exceed 246°. It appears that in all these systems, the sizeable dispersion forces associated with the indirect $I \cdots I$ contacts can favor these apparently surprising arrangements around the halide anion. Another remarkable point is also the coordination number around the halide anion, often found at 2 or 3, but easily extended to 6 as observed in the cubic structures described here (Szell *et al.*, 2017; Lieffrig *et al.*, 2013), and even to 8 in the co-crystal formed with CBr_4 as halogen-bond donor and $Me_4N^+Br^-$ (Lindeman *et al.*, 2003). Note that in the latter and despite an apparent crowding around the bromide anion, the reduction ratio for the $(Br_3C-)Br \cdots Br^-$ distance still amounts to 0.88, indicating a sizeable halogen-bond interaction.

Last but not least, the paper by Szell *et al.* (2017) in this issue also combines these crystal structures analyses with complementary solid-state NMR investigations. The formation of the honeycomb network from $Et_3BuN^+Br^-$ and (2) is indeed associated with a clear and substantial shift (+18/

35 p.p.m.) in the resonance of the carbon directly bonded to iodine, as a result of halogen-bond formation, in agreement with established trends in ^{13}C shifts of aromatic *ipso* C atoms upon halogen bonding (Moss & Goroff, 2005; Viger-Gravel *et al.*, 2013). Furthermore, $^{35/37}Cl$ and $^{79/81}Br$ solid-state NMR spectroscopy has also been used successfully to discriminate different coordination patterns of the Cl^- and Br^- anions, from approximately linear to distorted square planar to octahedral (Viger-Gravel *et al.*, 2014). These last results illustrate how the halogen-bonding interaction, whose renewal in the 1990s was essentially rooted in crystal engineering studies, is now diffusing into all areas of chemistry (Cavallo *et al.*, 2016), from theoretical and analytical investigations (in gas, liquid and solid states) to the optical, magnetic and conducting properties of crystalline materials, from soft matter issues (liquid crystals, polymers and gels) to biomolecular systems and their relevance to the pharmaceutical field.

References

Arunann, E., Desiraju, G. R., Klein, R. A., Sadlej, A., Scheiner, S., Alkorta, I., Clary, D. C., Crabtree, R. H., Dannenberg, J. J., Hobza, P., Kjaergaard, H. G., Legon, A. C., Mennucci, B. & Nesbitt, D. J. (2011). *Pure Appl. Chem.* **83**, 1637–1641.
Cavallo, G., Metrangolo, P., Pilati, T., Resnati, G., Sansotera, M. & Terraneo, G. (2010). *Chem. Soc. Rev.* **39**, 3772–3783.
Cavallo, G., Metrangolo, P., Milani, R., Pilati, T., Priimagi, A., Resnati, G. & Terraneo, G. (2016). *Chem. Rev.* **116**, 2478–2601.
Colin, M. (1814). *Ann. Chim.* **91**, 252–272.
Desiraju, G. R., Ho, P. S., Kloo, L., Legon, A. C., Marquardt, R., Metrangolo, P., Politzer, P., Resnati, G. & Rissanen, K. (2013). *Pure Appl. Chem.* **85**, 1711–1713.
Fourmigué, M. (2009). *Curr. Op. Solid State Mater. Sci.* **13**, 36–45.
Gilday, L. C., Robinson, S. W., Barendt, T. A., Langton, M. J., Mullaney, B. R. & Beer, P. D. (2015). *Chem. Rev.* **115**, 7118–7195.
Grebe, J., Geiseler, G., Harms, K. & Dehnicke, K. (1999). *Z. Naturforsch. B*, **54**, 77–86.
Lieffrig, J., Jeannin, O. & Fourmigué, M. (2013). *J. Am. Chem. Soc.* **135**, 6200–6210.
Lindeman, S. V., Hecht, J. & Kochi, J. K. (2003). *J. Am. Chem. Soc.* **125**, 11597–11606.
Metrangolo, P., Meyer, F., Pilati, T., Resnati, G. & Terraneo, G. (2008a). *Angew. Chem. Int. Ed.* **47**, 6114–6127.
Metrangolo, P., Meyer, F., Pilati, T., Resnati, G. & Terraneo, G. (2008b). *Chem. Commun.* pp. 1635–1637.
Moss, W. N. & Goroff, N. S. (2005). *J. Org. Chem.* **70**, 802–808.
Szell, P., Gabidullin, B. & Bryce, D. (2017). *Acta Cryst.* B**73**, 153–162.
Triguero, S., Llusar, R., Polo, V. & Fourmigué, M. (2008). *Cryst. Growth. Des.* **8**, 2241–2247.
Viger-Gravel, J., Leclerc, S., Korobkov, I. & Bryce, D. L. (2013). *CrystEngComm*, **15**, 3168–3177.
Viger-Gravel, J., Leclerc, S., Korobkov, I. & Bryce, D. L. (2014). *J. Am. Chem. Soc.* **136**, 6929–6942.